Surface Heat Transfer Measurements of a Scaled Serpentine Cooling Passage by Use of a Transient Liquid Crystal Technique

Ken-ichi Funazaki and Kouhei Ishizawa
Department of Mechanical Engineering
Iwate University
Morioka, Japan

Shigemichi Yamawaki
Aero-Engine and Space Operation
Ishikawajima-Harima Heavy Industries
Tokyo, Japan

ABSTRACT

This study is aimed at providing heat transfer characteristics of the three-pass serpentine cooling channel inside a 10:1 scaled model of an actual trubine blade. A transient method using Thermochromic Liquid Crystal (TLC) is employed to measure the surface heat transfer distribution inside the model. In this case it is important to pay an attention to the streamwise decrease in the mainstream temperature due to the heat absorption into the test model. To oversome this problem, the present study employed the linear interpolating method used by Ekkad and Han (1997) to estimate the local mainstream temperature. This study also conducts heat transfer measurements of straight-duct models with and without turbulence promoting ribs, which verifies the soundness of the measurement technique adopted in this study.

NOMENCLATURE

c	: specific heat
D	: hydraulic diameter
e	: rib height
h	: heat transfer coefficient
h_e	: heat transfer coefficeint based on the inlet temperature
Δh	: error in h
Nu_D	: Nusselt number (= hD/λ)
P	: rib pitch or periphery
Pr	: Prandtl number
Re_D	: Reynolds number (= UD/ν)
T	: surface temperature of the test model
T_g	: air bulk temperature of the main flow
$T_{g,e}$	: terminal temperature of the bulk temperature
T_i	: initial temperature of the test model
T_{ref}	: reference temperature
t	: elapse time from the onset of the measurement
U	: average velocity of the main flow
x	: streamwise direction of the cooling passage
y	: peripheral direction of the cooling passage

Greeks

λ	: thermal conductivity
$\tilde{\theta}$	: non-dimensionalized temperature
ν	: kinematic viscosity
ρ	: density
τ	: time constant
τ_j	: time lag of a small temperature rise

Subscripts

b	: air bulk

INTRODUCTION

To meet the demand for more accurate prediction of air-cooled turbine blade temperature, it has become a crucial issue to obtain quantitative information on heat transfer as well as aerodynamic behavior inside the serpentine cooling passage inside the turbine blade. Thanks to recent developments of CFD (Computational Fluid Dynamics) as well as rather surprising improvement in cost-performace of the computer, it has been becoming practical to predict the external heat transfer over the blade surface. However, as one can easily imagine, it is difficult to make an accurate analysis of the internal flow even with the application of the most sophisticated CFD codes because the internal flow contains very complicated flow events such as strongly swirling flow caused by 180 deg flow-turning at the bends, skewed flow separation due to inclined ribs attached on the inner surface of the passage. Nevertheless, several attemps are made to attack this cumbersome task. Abuaf and Kercher (1992) conducted the experimental and computationl studies on heat transfer as well as aerodynamic characteristics of the internal flow in a turbulated blade cooling passages. Abuaf and Kercher measured the heat transfer inside the scaled and transparent turbine blade model by use of the staedy-state liquid crystal technique and compared the data with the numerical evaluations obtained through a control-volume type flow solver using unstructured grids (STAR-CD). Abuaf and Kercher claimed that the CFD analyses of the heat transfer were in reasonable agreement with the experiments in

termes of area-averaged value. Unfortunately, they did not show any comparisons of the local heat transfer distributions between the calculations and the experiments, which would be necessary for verification of the solver and/or the grid system used. The present authors believe that CFD-aided design of the turbine blade cooling passage is a very promising approach, however, its success in the industries surely relies on the establishment of the database not only for the heat transfer but also for the aerodynamics inside the passages through well-organized experiments using a test model with realistic geometry.

This study is therefore aimed at providing some heat transfer data inside the serpentine passages of a 10:1 scaled model for an actual trubine blade. A transient technique using Thermochromic Liquid Crystal (TLC) is employed to measure the surface heat transfer distribution inside the model. In this case, as pointed out by Chyu et al. (1997), one should pay a great attention to the streamwise decrease in the mainstream temperature due to the heat absorption into the test model. To oversome this problem, several compensating methods have been proposed by some reserchers (Saabas et al. (1987), Chyu et al. (1997). The present study employed the linear interpolating method used by Ekkad and Han (1997) to estimate the local value of the mainstream temperature.

THEORETICAL BACKGROUND

Transient Method

Suppose that the heat conduction from the mainstream into the body concerned is one-dimensional, the surface temperature of the body subjected to a sudden increase in main flow temperature is governed by the following equation:

$$\tilde{\theta}(t) \equiv \frac{T(t) - T_i}{T_g - T_i} , \tag{1}$$

$$\tilde{\theta}(t) = 1 - \exp\left(\frac{h^2 t}{\rho c \lambda}\right) \mathrm{erfc}\left(\frac{h\sqrt{t}}{\sqrt{\rho c \lambda}}\right) , \tag{2}$$

where h is a heat transfer coefficient and an unknown vaiable in this case. In practice, however, the main flow temperature usually exhibits some asymptotic behavior rather than sudden change. Application of the Duhamel's theorem provides an approximate expression for the temperature increase of the body surface. In case the main flow temperature is approximated by stepwise increases as shown in Figure 1, we have a following expression for the time-varying surface temperature.

$$T(t) - T_i = \sum_{j=1}^{N} U\left(t - \tau_j\right)\left(T_g - T_i\right)_j , \tag{3}$$

$$U\left(t - \tau_j\right) = 1 - \exp\left[\frac{h^2\left(t - \tau_j\right)}{\rho c \lambda}\right] \mathrm{erfc}\left[\frac{h\sqrt{\left(t - \tau_j\right)}}{\sqrt{\rho c \lambda}}\right] , \tag{4}$$

where N is the number of the steps and τ_j is the time lag of the j-th step measured from the onset of the measurement. The other ways of the approximation could be possible likewise in the study of Saabas et al. (1987) using the several linear segmentations, for example.

Provided that the time history of the surface temperature $T(t)$ is known, it is easy to determine the heat transfer coefficient h from Eq. (1) or Eq. (3) through an iteration method. In this case an attention has to be paid to the one-dimensionality of the heat conduction at the location concerned. Several studies were already made on this point. Onuki (1997) found from the study on a rib-roughened surface using FDM that in most cases one could not expect the one-dimensionality very near the rib due to its fin-effect. It must be the case for the corner region of an internal cooling passage.

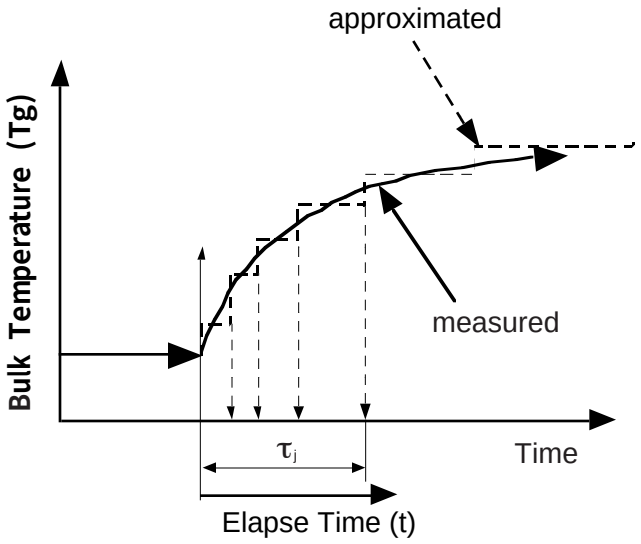

Figure 1 Schematic of a time history of mainstream temperature and its step-like approximation

Streamwise Variation of Main Flow Temperature

Applying the above-mentioned transient method to an internal cooling passage, one should pay a great attention to the streamwise variation of the main flow temperature. It is because the test model absorbs thermal energy from the main flow, resulting in decreasing bulk temperature of the main flow. Therefore if no correction is made, the heat transfer coefficient is always underestimated due to the larger temperature difference $T_g - T_i$ than should be. Chyu et al. (1997) examined several approaches to overcome this difficuly and proposed a method to correct the local heat transfer coefficient h_e that was determined by assuming constant air bulk temperature throughout the cooling passage. In principle their method derived the local air bulk temperature $T_b(t,x)$ on a basis of the thermal energy balance, which can be written as follows:

$$\left(\rho c_p U\right)_g A\left(T_e(t) - T_b(t,x)\right) = \int_0^{P\,x}\int_0^{P} dq = \int_0^{P\,x}\int_0^{P} h_e\left(T_e(t) - T_w(t,x,y)\right) dxdy . \tag{5}$$

Eq. (5) requires the peripheral distribution of the heat transfer coefficient over the integral domain. Actually, however, it is quite difficult to obtain the perferal heat transfer distribution from a single experiment because such a measurement necessitates an observation using several video cameras at the same time. To make matters worse, it is highly possible that some areas can not be seen from the outside, especially in the case of multipass-type models that are of interest in this study.

One of the practical ways to evaluate the local bulk temperature is to measure the time-varying main flow temperature at several locations in the passage and interpolate them, which was already adopted by

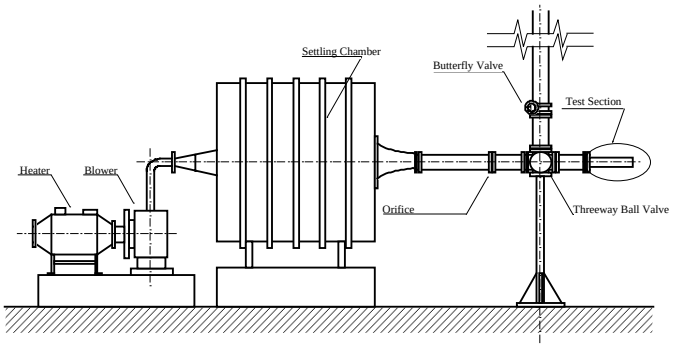

Figure 2 Test apparatus

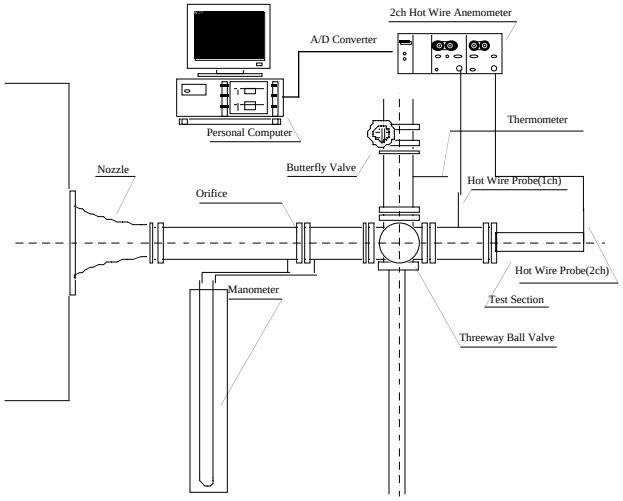

Figure 3 Test section and measurement system

Ekkad and Han (1997). Ekkad and Han used the linear interpolation in their study on heat transfer measurement of a twopass-type passage. The present study employs basically the same approach as that of Ekkad and Han. In this case one must be careful whether the measured main flow temperature is truly the bulk temperature as pointed out by Chyu et al. (1997).

TEST APPARATUS

Wind Tunnel

Figure 2 shows the test apparatus used in this study. Figure 3 represents the detailed description of the test section and the flow-switching section, including the measurement system. Air was preheated by an electric heater before entering the blower. Flow rate, regulated by the inlet valve of the blower, was measured by an orifice plate (JIS Z 8762). The present study examined two serpentine-passage models, of which geometries are described later. Three straight-duct models of square cross section with and without turbulence promotors were also employed to check the validity of the measurement technique developed in this study. Each of the test models was attached to the horizontal exit of the diverging valve. Prior to starting the heat transfer measurement of the test model, the heated air was kept been discharged from the vertical exit of the valve via the diverging valve until the air temperature reached the equilibrium state. In this case a butterfly valve, connected

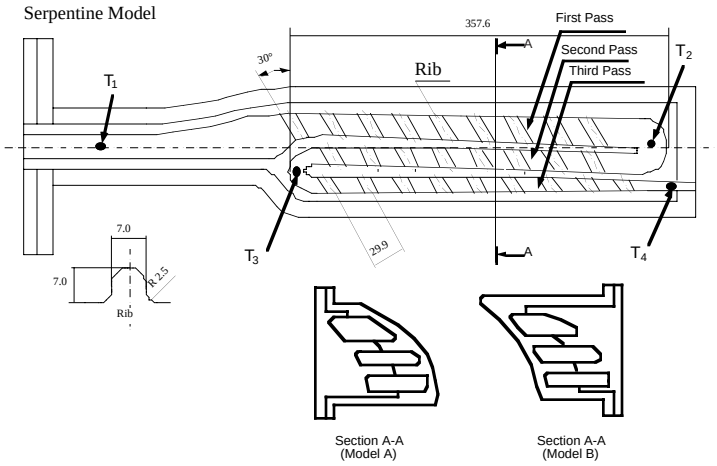

Figure 4 Serpentine Passage Models and their cross sections at the mean radius

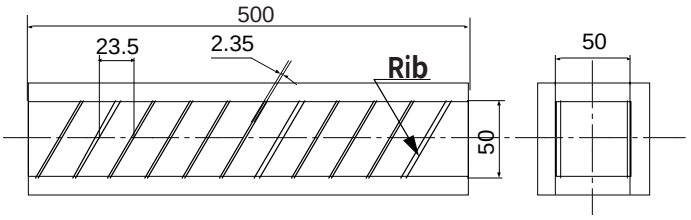

Figure 5 Straight-duct model with turbulators (In-line model) adoped for checking the soundness of the present technique

to the vertical exit of the diverging valve, was carefully adjusted so that the flow rate through the orifice did not change after switching the flow direction. Although the diverging valve was operated manually, it took less than half a second to change the flow direction completely.

Test Model

Figure 4 shows the serpentine passage models with their cross sections at the mean radius, which were 10X-scaled models of the HP turbine blade of an aero-engine. These two models, designated 'Model A' and 'Model B' respectively, had different external profiles, while the internal structures of the models were identical with each other consisting of three rib-roughened cooling passages. With a great care to their transparency, they were all machined from the acrylic-resin block except for the ribs. Actually the ribs were glued on the inner surfaces of the serpentine models, which resulted in deterioration of the transparency at the glued area.

Prior to the heat transfer measurement of the srpentine model, straight-duct models as shown in Figure 5 were used to check the soundness of the measurement technique developed in this study. Two types of straight-duct model adopted were 500mm long and had 50mm x 50mm square cross sections. One of them consisted of four smooth walls and the other model had rib-roughened walls of in-line rib configuration. The latter model, with rib height ratio $e/D = 0.047$ and rib pitch ratio $P/e = 10$, were made to be almost identical with the test model of Han and Park (1997) for comparing the data obtained through the present TLC method with the thermocouple-based experiments done by Han and Park.

Instruments and Image Processing

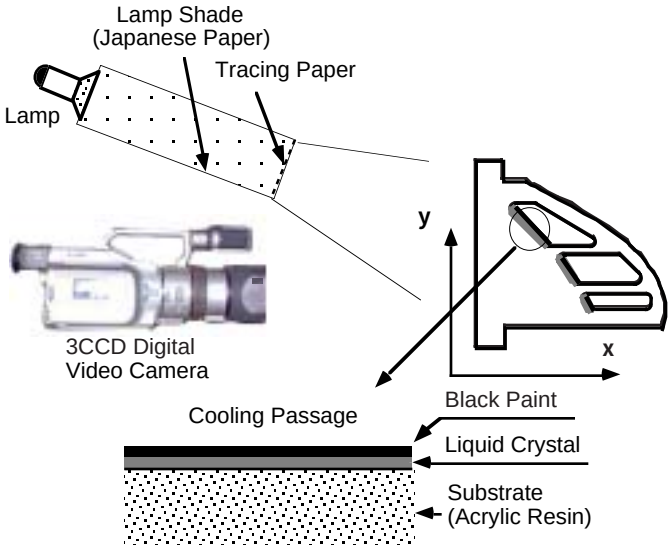

Figure 6 Setup for the transient measurement of the local heat transfer by use of TLC

Instantaneous air temperatures at the inlet and outlet of the test model were monitored by two 'cold-wire' probes that were connected to an anemometer operating at constant-current mode. A high-speed A/D converter in the PC acquired the temperature data. Thermocouples for measuring the mainstream temperature were also embedded at the locations designated T_1, T_2, T_3 and T_4 in Figure 3. Signals from the thermocouples were captured by a computer-controlled data logger.

Figure 6 demonstrates the setup for the transient measurement of the surface heat transfer for the Model A by use of TLC. A narrow-band TLC was sprayed on the rib-roughened surfaces opposite with the flat external surface of the model in order to get a clear view of the color pattern of the TLC. The temperature range of the TLC used was nominally 32 °C- 34 °C. Color images of the TLC were captured and recorded in NTSC format by a 3 CCD digital video camera (SONY VCR-VX1000). This camera was able to hold the images of digitally on a magnatic tape at the video frame rate (e.g. 30 frames per second), making it possible to keep a number of color images. The maximum size of ech of the images was about 350,000 pixels. Time records of the images were also written on the tape, from which one could determine the elapse time of each of the images from the beginning of the measurement. The video camera could transfer a clear still picture frame by frame, which enabled the PC (PowerMacintosh) to grab the RGB image file as described later. Lighting was another key factor in the measurement. Although the optical axes of three halogen lamps used were at some angle with the flat surface of the test model , the reflection of the light could not be completely avoided, which restricted the viewable area of the inner passages. The lamps were therefore wrapped with the paper shades to scatter the light, which could ease the difficulty associated with the lighting to some extent.

Figure 7 exhibits the procedure for image processing. A commercial application for image processing (Adobe Photshop) running on a PC (PowerMacintosh) grabbed RGB images of the liquid crystal frame by frame via the NTSC-formatted signal transmitted from the video camara. It could also make hue images of 8 bit resolution from the RGB data, which were used to detect the iso-thermal contours through the calibration data correlating a surface temperature with the color (hue

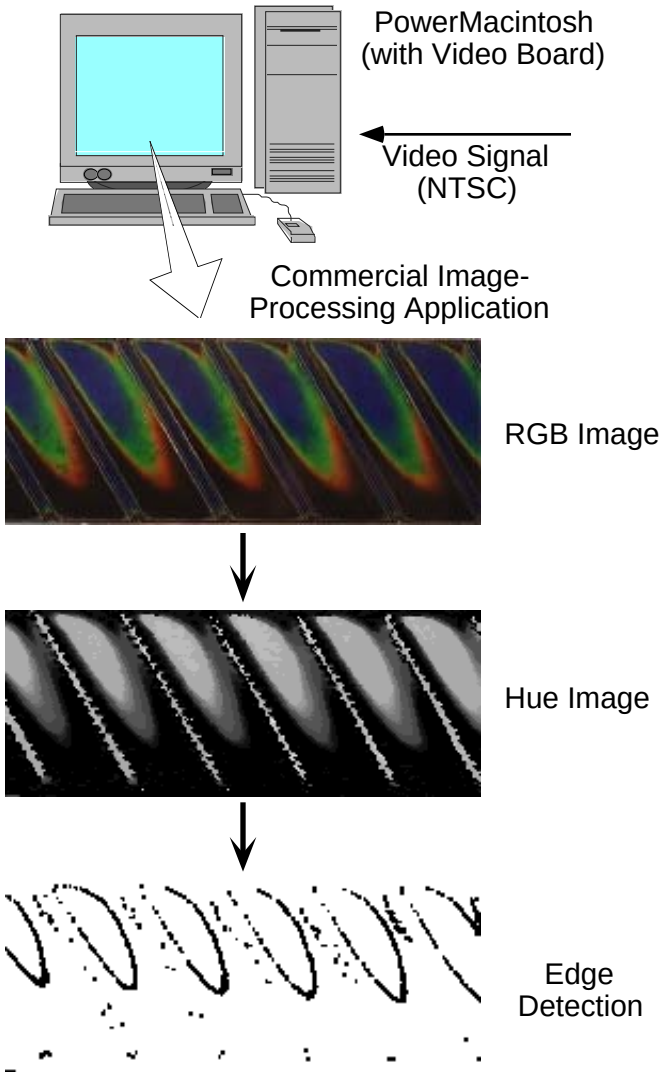

Figure 7 Procedure for image processing by use of a commercial application to detect the edges of the specified color (hue)

value) of the TLC.

Calibration

A calibration was made to identify the temperature of the target color (hue value). The target color was green and its hue value was 97 in the range between 0 and 255 (8 bit). The details of the setup for the calibration was documented by Ishizawa (1996). The calibration was executed in a very similar manner with the actual measurement in terms of the configuration of the test model and the lighting devices. This calibration also investigated a dependency of the temperature-hue relationship upon the angle between the optical axis and the surface of the test model, which was indispensable information in the case of the serpentine model because the surface to be measured was inevitably inclined at some angle against the optical axis of the vedio camera.

Through the calibration, it followed that the reference temperature T_{ref} corresponding to the reference hue value was $33.4\,°C \pm 0.05\,°C$. The angle dependency of the refernce temperature was shown in Figue

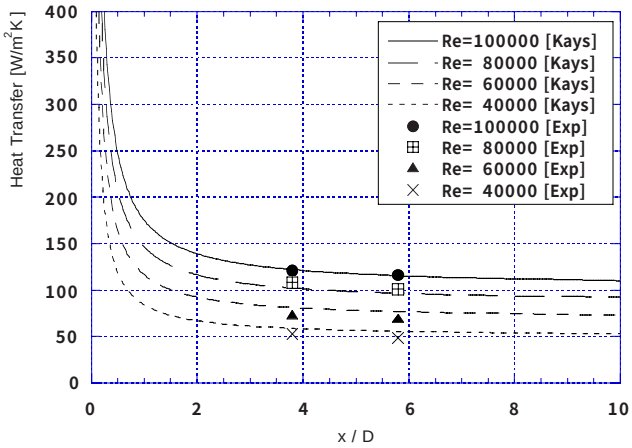

Figure 8 Comparisons of heat transfer cofficient between the corrlation (Kays and Crawford) and the experiments for the smooth duct

Uncertainty

In the transient method, a heat transfer coefficeint h is not given in an explicit form, causing some difficulty in estimation of uncerainty associtaed with the measured heat transfer coefficient. According to Saabas et al. (1987), an error in h can be calculated by the following relationship:

$$\Delta h = \frac{\frac{\partial \tilde{\theta}}{\partial T}\Delta T + \frac{\partial \tilde{\theta}}{\partial T_g}\Delta T_g + \frac{\partial \tilde{\theta}}{\partial T_i}\Delta T_i - \frac{\partial \tilde{\theta}}{\partial t}\Delta t - \frac{\partial \tilde{\theta}}{\partial k}\Delta k}{\partial \tilde{\theta}/\partial h}, \qquad (6)$$

which is obtained from Eqs. (1) and (2) , where $k = \rho c \lambda$ and variables with Δ represent errors associated with the parameters used. Neglecting the fact that all errors are not stochastic, one can evaluate the uncertainty of the heat transfer coefficient as follows:

$$\Delta h = \frac{\sqrt{\left(\frac{\partial \tilde{\theta}}{\partial T}\Delta T\right)^2 + \left(\frac{\partial \tilde{\theta}}{\partial T_g}\Delta T_g\right)^2 + \left(\frac{\partial \tilde{\theta}}{\partial T_i}\Delta T_i\right)^2 + \left(\frac{\partial \tilde{\theta}}{\partial t}\Delta t\right)^2 + \left(\frac{\partial \tilde{\theta}}{\partial k}\Delta k\right)^2}}{\partial \tilde{\theta}\ \partial h} \qquad (7)$$

where the sensitivities such as $\partial \tilde{\theta}/\partial T$ can be derived from Eq. (1) or Eq. (2). Substitution of the parameters used into Eq. (7) yields that uncertainty in h was about 5% for the case of the straight-duct model eith no ribs. As for the rib-roughened model or the serpentine model, the relevant discussions on the uncertainty are given in the following section.

RESULTS

Straight-Duct Model

Figure 8 shows the experimental heat transfer coefficeints obtained along the center line of the smooth-duct model with no rounded fillet at the entrance, which are compared with the correlation given by Kays and Crawford (1980). The correlation is expressed as follows, in consideration of the entrance effect (Yeh et al. (1984)):

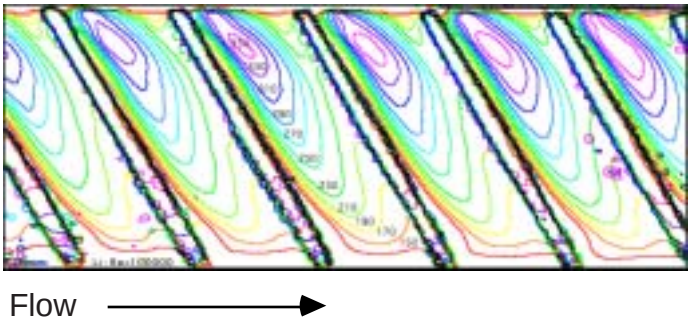

Figure 9 A typical result of iso-heat transfer contours for the rib-roughened straight-duct model, $Re_D = 100,000$

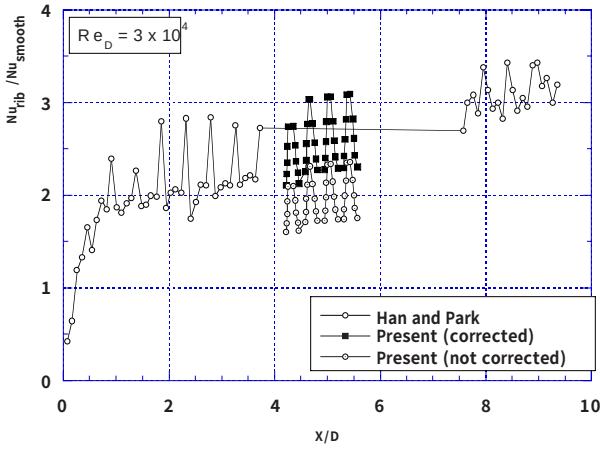

Figure 10 Comparisons of heat transfer cofficient for the rib-roughened duct model between the data of Han and Park and the present measured data with and without bulk temperature

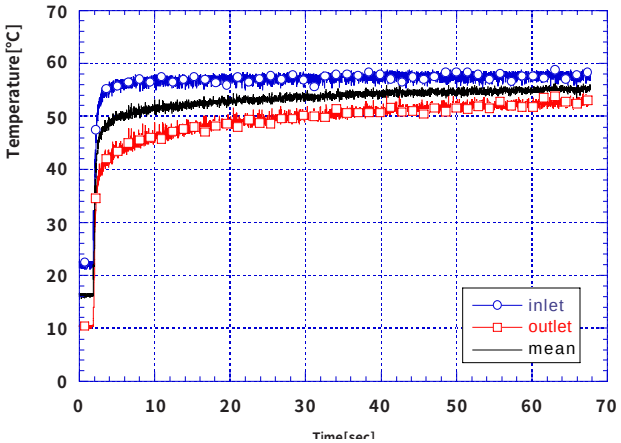

Figure 11 Instantaneous temperatures at the inlet and outlet of the rib-roughened duct model measured by cold-wire probes

$$Nu_D = \left(1 + 0.7\frac{D}{x}\right) Nu_{D,\infty}, \qquad (8)$$

$$Nu_\infty = 0.022 Re_D^{0.8} Pr^{0.5}, \qquad (9)$$

where x is the distance from the entrance. Note that the main flow temperature did not show any drastic change inside the test model in this case. It follows from Figure 8 that the measured heat transfer coefficients almost matched the correlation.

Figure 9 demostrates the measured heat transfer data for the rib-roughened straight-duct model with $Re_D = 100,000$. As several studies revealed, peak values of the heat transfer measured between two neighboring ribs appeared near the upper smooth side wall that met the ribs at an acute angle. Figure 10 shows two heat transfer coefficient distributions along the center line of the rib-roughened duct model measured by the present authors as well as by Han and Park (1986) for $Re_D = 30,000$. Note that Han and Park employed steady-state approach to obtaine the heat transfer using thermocouples. In this case the Nusselt number was normalized with the value given by Eq. (7). Also shown is the heat transfer coefficient determined without any air bulk temperature correction, for comparison. Although the present measurement did not cover the region that was examined by Han and Park, the obtained data were in a quantitative accordance with the data of Han and Park. As mentioned above, the heat transfer with no correction was lower than the corrected one. This was because the heat transfer was so enhanced by the ribs that the main flow temperature considerably decreased while passing through the test model, as shown in Figure 11. This figure shows time histories of the inlet and outlet temperatures measured with the cold-wire probes, revealing that the outlet temperature changed with the elapsed time in a relatively gradual manner compared to the inlet temperature. Since the observed region was around at the middle of the test model, the local bulk temperature to estimate the heat transfer was calculated simply by averaging the two measured temperatures, which is also shown in Figure 11. Since the error associated with the averaged air bulk temperature was more or less 1 K, uncertainty in the heat transfer coefficient based on the averaged air bulk temperature was about 10%.

Serpentine Model

Figure 12 demonstrates the heat transfer distributions of the serpentine passage model ('Model A'), where the Reynolds number based on the inlet hydraulic diameter and inlet velocity was about 23000. Figure 13 shows unsteady temperatures measured by the four thermocouples at the four locations inside the passage of the serpentine model (see Figure 4). Due to the heat-absorbing effect of the test model, the measured air temperature gradually decreased towards the exit of the passage. Heat transfer coefficients shown in Figure 12 were

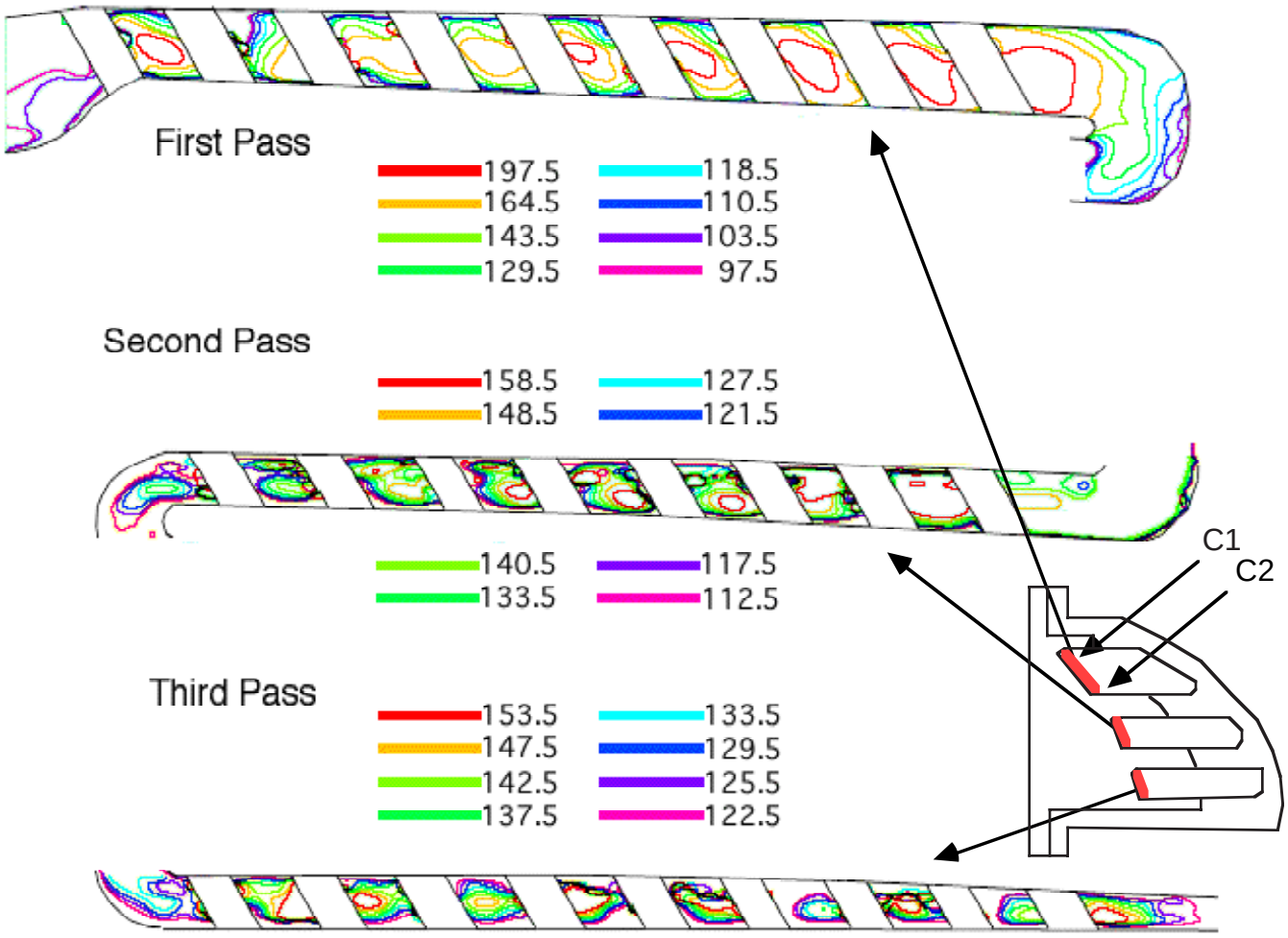

Figure 12 Heat trasnfer distributions of the serpentine passage model (Model A)

calculated separately for each of the three passes, where for the sake of simplicity the mean air bulk temperatures were used as the main stream temperature for the three passes, respectively. This means that heat transfer coefficients on the upstream side of each of the passes were underestimated due to the overestimated temperature difference $T_g - T_i$, and were overestimated for the downstream sides of the passes. Accordingly uncertainty in h measured was about 10% near the middle of the passes and about 18% at the most upstream or downstream location was 18%.

In the first pass of the test model, peak values of the heat transfer coefficient appeared near the pass center line. Despite the same rib angle to the flow direction, this was in contrast with the case of the rib-roughened straight-duct model as seen in Figure 9, where the peak values occurred near the upper side wall. There are two reasons for this difference. One is the difference in rib shape. In the straight-duct model, the cross section of the rib was square, whereas the serpentine model used rounded ribs as turbulator. The other reason, which seems more plausible for the authors, is the difference in the shape of the passage cross section. As seen in Figure 13, the cross section of the first pass of the serpentine model was not a rectangular but a deformed trapezoidal . The measured surface met the upper smooth wall at an acute angle at the corner marked as C_1 and the flow area were relatively narrow compared to the flow area at the corner marked as C_2, which seemingly caused the downdard shift of the locations of the peak values. After the 180 deg turn after the first pass, due to the secondary flow and the associated high turbulence there arised considerably high heat transfer regions in the second pass, followed by heat transfer peaks appearing behind the ribs at the locations as expected from the data for the ribbed straight-duct model. One might also notice that the other peaks occurred at the opposite side of the pass. It seems that they could be attributed to the secondary flow generated at the first 180 deg turn, however, further investigations are needed for them. Few remakable events happened in the third pass, which was probably due to the quite high turbulence intensity caused by the accumulation of the turbulence energy generated at the upstream passes and turns, as reported in Abuaf and Kercher (1994) for their serpentine model.

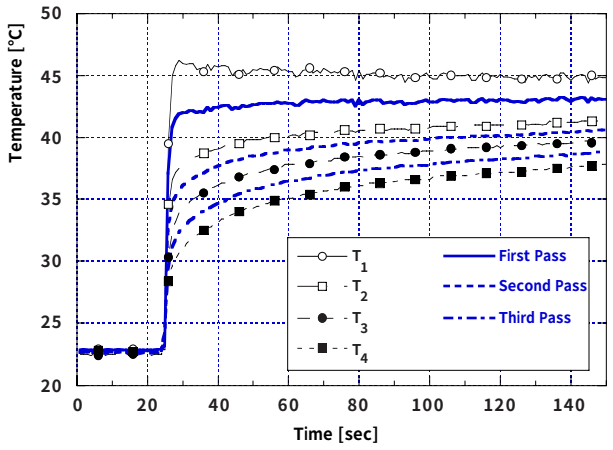

Figure 13 Time-varying temperatures at thefour locations inside the serpentine model measured by thermocouples

DISCUSSION

As described in the above, the linear interpolation technique, which was used in this study to evaluate the local air bulk temperature, resulted in significant error in the measured heat transfer coefficient. To overcome this problem without installing further thermocouples into the test model or employing extra devices, the following procedure is now being developed on a basis of the teechnique of Gillespie et al. (1996).

When a local air bulk temperature in the inner cooling passage varies with time according to the next relationship,

$$T_g = T_i + \left(T_{g,e} - T_i\right)\left(1 - e^{-t/\tau}\right), \tag{10}$$

the temperature on the test surface subjected to the air follows the curve given by (Gillespie et al. (1996))

$$\frac{T - T_i}{T_{g,e} - T_i} = 1 - \frac{\frac{\rho c\lambda}{h^2\tau}}{1 + \frac{\rho c\lambda}{h^2\tau}} \exp\left(\frac{h^2 t}{\rho c\lambda}\right) \operatorname{erfc}\left(\frac{h\sqrt{t}}{\sqrt{\rho c\lambda}}\right)$$
$$- \frac{\exp(-t/\tau)}{1 + \frac{\rho c\lambda}{h^2\tau}} \left(1 + \frac{\sqrt{\rho c\lambda}}{h\sqrt{\tau}}\left(\frac{1}{\pi}\sqrt{\frac{t}{\tau}} + \frac{2}{\pi}\sum_{n=1}^{\infty}\frac{1}{n}\exp\left(-\frac{n^2}{4}\right)\sinh n\sqrt{\frac{t}{\tau}}\right)\right) \tag{11}$$

Provided that a time constant of the temeprature change with time is known, unknowns in the above expression are a terminal temprature $T_{g,e}$ and a heat transfer coefficient, which can be determined in principle from the two sets of elapse time (t) and reference temperature (T). However, time constant τ is not unique in the flow field as seen in Figure 13. Therefore it is necessary to consider τ as the third unknown parameter, which requires at least one more data set of elapse time and reference time to solve the resultant simultaneous equations. This technique, so called multi-index color techinque,

CONCLUSIONS

The present study was executed aiming at providing heat transfer characteristics of the three-pass serpentine cooling channel of an actual trubine blade, in conjunction with the heat transfer data of rib-roughened straight-duct model for verfication of the measuring technique. The contents of this paper is itemized as follows:

(1) The linear interpolation of the time-varying temperature data measured at several points in the test channel was employed to estimate the local air bulk temperature. The temperature measurement utilized 'cold-wire' probe of the anemometer as well as thermocouples.

(2) In the experiments using straight-duct model with no ribs the measured heat transfer data almost matched the correlation. In the case when the air bulk temperature was properly corrected, the heat transfer data for the rib-roughened duct model also exhibited a good agreement with the data obtained by Han and Ekkad.

(3) In the first pass of the serpentine model peak values of the heat transfer associated with the angled ribs occurred in a different manner from those of the straight-duct model, which could be attributed mainly to the deformed cross section of the channel of the first pass.

(4) After the first bend of the channel in the serpentine model, relatively high heat transfer regions appeared seemingly due to the secondary flow generated in the bend. Peak values of the heat transfer in the second pass occurred at the locations behind the ribs likewise in the case of the straight-duct model.

(5) In the third pass, notable features of the heat transfer distribution between the ribs could not be identified because of the intense turbulence enhanced by the bends and ribs.

ACKNOWLEDGMENTS

The authors are greatly indebted to K. Sasaki of Technical Center of Iwate University for his help in manufacturing the test facility.

REFERENCES

Abuaf, N. and Kercher, D. M., 1992, "Heat Transfer and Turbulence in a Turbulated Blade Cooling Circuit," ASME Paper 92-GT-187., pp.

Chyu, M. K., Ding, H., Downs, J. P., Van Sutendael, M. and Soechting, F. O., 1997a, "Determination of Local Heat Transfer Coefficeint Based on BUlk Mean Temperature Using a Trasient LIquid Crystals Technique," ASME Paper 97-GT-489., pp.

Ekkad, S. V. and Han, J. C., 1997b, "Detailed Heat Transfer Distributions in Two-Pass Square Channels with Rib Turbulators," International Journal of Heat and Mass Transfer, Vol. 40, pp. 2525-2537.

Gillespie, D. R. H., Wang, Z., Irlend, T. and Kohler, S. T., 1996, "Full Surface Local Heat Transfer Coefficient Measurements in a Model of an Integrally Cast Impingement Cooling Geometry," ASME Paper 96-GT-200., pp.

Han, J. C. and Park, 1986, "Measurement of Heat Transfer and Pressure Drop in Rectuanglar Channels with Turbulence Promotors," 4015, NACA.

Ishizawa, K., 1996, "Studies on Heat Transfer Measurements in the Turbine Cooling Passage by Use of Liquid Crystal," Bachelor Thesis, Iwate University.

Kays, W. M. and Crawford, M. E., 1980, "Convective Heat and Mass Transfer," McGraw-Hill, p. 140.

Onuki, A., 1997, "Numerical Studies on Transient Heat Conduction of a Rib-Roughened Surface," Bachelor Thesis, Iwate University.

Saabas, H. J., Arora, S. C. and Abdel Messeh, W., 1987, "Application of the Transient Test Technique to Measure Local Heat Trabsfer Coefficients Associated with Augmented Airfoil Cooling Passage," ASME Paper 87-GT-212., pp.

Yeh, F. C. and Stepka, F. S., 1984, "Review and Status of Heat-Transfer Technology for INternal Passages of Air-Cooled Turbine Blades," 2232, NASA.